Second International Conference on CFD in the Minerals and Process Industries
CSIRO, Melbourne, Australia
6-8 December, 1999

MODELLING OF FLOWS IN A LADLE WITH GAS STIRRED LIQUID WOOD'S METAL

J. L. XIA[1], T. AHOKAINEN[1], and L. HOLAPPA[2]

[1]Laboratory of Materials Processing & Powder Metallurgy,
[2]Laboratory of Metallurgy Helsinki University of Technology, PB 6200, FIN-02015, HUT, Espoo, FINLAND

ABSTRACT

The present paper describes a numerical study of two phase flows in a ladle with gas stirred liquid Wood's metal using the CFX code. A cylindrical model ladle containing the molten metal is considered, and nitrogen is injected vertically upward through a nozzle centrally located at the bottom. An Eulerian-Eulerian two phase model is used. The interface momentum exchange includes effects of drag, lift and turbulent dispersion forces. Different drag and lift force coefficients have been examined to find a reasonable set of values for these parameters. Predictions are compared against the experimental data measured in an identical model ladle (Xie et al, 1992a and 1992b) for the mean axial and radial liquid velocities, the bubble rising velocity, and gas volume fraction at various heights. Results show that the mathematical model can give a reasonable prediction of flows in the liquid region, but, a relatively large deviation exists in the gas-liquid plume, for the cases considered. The present results accumulate information of CFD in modelling two phase flows in molten metals.

Keywords: gas injection, molten metal, two phase flow, interface interaction, modelling

NOMENCLATURE

C's empirical constants in the turbulence model
C_D drag coefficient
C_L lift force coefficient
C_{TD} turbulent dispersion coefficient
d_b bubble diameter (m)
D ladle diameter (m)
E_o Eotvos number
F source term
g gravitational acceleration (m/s^2)
H bath height (m)
k turbulence kinetic energy (m^2/s^2)
p pressure (Pa)
r radius (m)
Re Reynolds number
u mean axial velocity (m/s)
u_i mean velocity in the x_i-direction (m/s)
u'_i velocity fluctuation in the x_i-direction (m/s)
v mean radial velocity (m/s)

Greek symbols
α volume fraction
ε dissipation rate of k (m^2/s^3)
μ dynamic viscosity (kg/ms)
μ_t turbulent viscosity
ρ density (kg/m^3)
σ empirical diffusion coefficients in turbulent model

Subscripts
i, j spatial co-ordinates
g gas
l liquid

INTRODUCTION

Gas injection is a common practice in metallurgical processes to enhance reaction, to eliminate thermal and/or composition gradients, to remove inclusions and others. For example, submerged gas injection plays a vital role in copper and aluminium industries. This leads to intensive experimental and numerical investigation. Brimacombe et al. (1990) conducted a comprehensive review on industrial development and fundamental research on gas-liquid interaction in various metallurgical processes. Mazumdar and Guthrie (1995) summarised experimental and numerical work on the important and specific applications of gas stirring in ladle metallurgy steel making operations. Other reviews include those by Mori (1988) who dealed mainly with kinetic investigations on fundamental reactions related to steelmaking processes, and by Evans (1997) who focused on recent CFD research work on gas-stirred melts and continuous casting.

Most of the past investigations have been made for aqueous systems, and sparse work has been done on the flow fields of the molten metals, especially numerical modelling of flows in molten metals with comparison of flow fields and plume behaviour with experimental measurements is lacking. Obviously, one should be careful to extrapolate the results of water model to the practical molten metal systems because the physical properties of the liquid exert considerable effect on jet behaviour (Oryall & Brimacombe, 1976) while the properties of water are quite different from those of liquid metals. Xie et al. (1992a and 1992b) made detailed measurements for gas stirred molten metal using a low-melting-point alloy called Wood's metal as a modelling liquid. In their study, flow velocities and bubble behaviour in a model ladle with liquid Wood's metal under various blowing conditions were measured using magnet probe and double-contact electro-resistivity probe. Data were presented in the form of axial and radial liquid velocities, turbulence kinetic energy, Reynolds stresses, and gas volume fraction at various

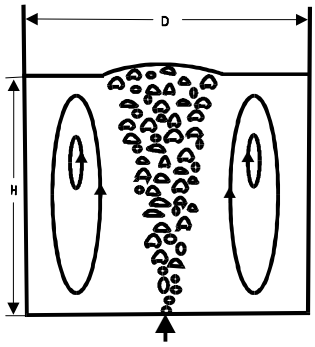

Figure 1: Schematic of a model ladle with

heights. The bubble plume behaviour and flow velocity in gas stirred liquid Wood's metal were also reported for an eccentric nozzle position by Xie and Oeters (1994). Turkoglu & Farouk (1992) carried out a numerical calculation for the flow in a ladle with gas-stirred liquid metals. However, no detailed comparison of the flow velocity and the plume characteristics with experimental data was made. This is essential to validate the numerical prediction and the mathematical models used. For the interface momentum exchange, they took the drag force into account and discarded the lift force and the turbulent dispersion force, which should have strong effect on phase distribution, as it has been shown by other researchers (e.g., Legendre & Magnaudet, 1998, Davidson, 1990).

The present study is to use the Eulerian two phase approach to numerically simulate flows in a model ladle with nitrogen stirred liquid Wood's metal and make a critical assessment of the mathematical models via detailed comparison with experiments of Xie et al. (1992a and 1992b) so as to accumulate information of CFD in modelling the molten metal systems in metallurgical processes.

MATHEMATICAL MODEL

The physical problem considered is a model ladle with liquid Wood's metal which is agitated by injected nitrogen from a nozzle centrally located at the bottom, as sketched in Fig. 1. The model ladle is of diameter 400 mm, filled with the liquid Wood's metal to a depth of 370 mm. A nozzle with a diameter of 3 mm is located at the central bottom, flush with the surface, to inject nitrogen, a modelling gas. The injection flow rate is 200 Ncm^3/s. Experimental measurements have been done in an identical model ladle by Xie et al (1992a, 1992b) for the flow behaviour of both liquid and gas phases at various heights to allow to evaluate the numerical predictions in detail. The density and the viscosity of the Wood's metal are closer to the values of the liquid iron than those of water and mercury, though its surface tension is lower than that of iron but is much higher than that of water. Thus the performance from the Wood's metal system should be closer to the practical molten metal systems.

Governing Equations

An Eulerian-Eulerian two phase model is used for the present simulation. Molten metal and gas are treated as two different continuous phases interpenetrating and interacting with each other. On the same Eulerian cell, the same pressure in both phases is assumed, and flow equations for each phase are weighted by their volume fraction. Besides the drag force, the lift force and the turbulent dispersion force are taken into consideration for the interface interactions. A complete analysis of two phase flow induced requires solution of the mass and momentum conservation equations over the flow domain and use of appropriate boundary conditions for each phase.

For steady and isothermal flow, the conservation equations may be described in Cartesian tensor as follows:

for the continuous (liquid) phase,

$$\frac{\partial(\alpha_l \rho_l u_{lj})}{\partial x_j} = 0 \tag{1}$$

$$\frac{\partial(\alpha_l \rho_l u_{li} u_{lj})}{\partial x_j} = -\alpha_l \frac{\partial p}{\partial x_i} + \frac{\partial}{\partial x_j}\left[\alpha_l \mu_l \left(\frac{\partial u_{li}}{\partial x_j} + \frac{\partial u_{lj}}{\partial x_i}\right)\right] - \frac{\partial(\alpha_l \rho_l \overline{u'_{li} u'_{lj}})}{\partial x_j} + \alpha_l(\rho_l - \rho_o) g_j + F_{lj} \tag{2}$$

For dispersed (gas) phase,

$$\frac{\partial(\alpha_g \rho_g u_{gj})}{\partial x_j} = 0 \tag{3}$$

$$\frac{\partial(\alpha_g \rho_g u_{gj} u_{gj})}{\partial x_j} = -\alpha_g \frac{\partial p}{\partial x_i} + \frac{\partial}{\partial x_j}\left[\alpha_g \mu_g \left(\frac{\partial u_{gi}}{\partial x_j} + \frac{\partial u_{gj}}{\partial x_i}\right)\right] - \frac{\partial\left(\alpha_g \rho_g \overline{u'_{gi} u'_{gj}}\right)}{\partial x_j} + \alpha_g(\rho_g - \rho_o) g_j + F_{gj} \tag{4}$$

F_l and F_g consist of phase interactions which cause the transfer of momentum between relatively moving phases. Here the drag, lift, and the turbulent dispersion forces are taken into account. The drag force is calculated as follows (Cook & Harlow, 1983, Davidson, 1990):

$$F_l^D = -F_g^D = \frac{3C_D}{4d_b}\alpha_g \rho_l \left|\vec{u}_g - \vec{u}_l\right|(\vec{u}_g - \vec{u}_l) \tag{5}$$

C_D is the drag coefficient which varies with flow conditions. For a bubble with 20 mm in diameter, anticipating a relative velocity between the phases as 0.35 m/s, it is estimated the bubble Reynolds number Re=1.56×10^4. This indicates that the flow is in turbulent

region. In this region, C_D is independent of Reynolds number.

When bubbles rise in a liquid, in which there exists a mean velocity gradient, they will be subject to a lift force down to the velocity gradient due to the unequal pressures on the two sides of the bubble. This lift force is proportional to the relative velocity between the phases and the local liquid vorticity. For a bubble swarm, it may be computed from the following relation (Drew & Lahey, 1987):

$$F_l^L = -F_g^L = \rho_l \alpha_g C_L \left(\vec{u}_g - \vec{u}_l\right) \times curl\vec{u}_l \qquad (6)$$

here the lift force coefficient C_L can take values between 0.01 and 0.5. In the present study, it is set as 0.1 for an average 6 mm diameter bubble and 0.15 or 0.3 for an average 20 mm diameter bubble.

The effect of the dispersion of bubbles in turbulent liquid flow is taken into account according to the following expression proposed by Lopez de Bertodano (1992) for the turbulent dispersion force:

$$F_l^{TD} = -F_g^{TD} = \rho_l k_l C_{TD} \nabla \alpha_l \qquad (7)$$

This means that the turbulent dispersion force depends on the amount of turbulence in the liquid phase and the gradient of the volume fraction. The turbulent dispersion coefficient C_{TD} is set to 0.1.

The total conservation requires:

$$\alpha_l + \alpha_g = 1 \qquad (8)$$

Turbulence is modelled by the *k-ε* high Reynolds number turbulence model (Launder & Spalding, 1974), and the Reynolds stresses are then given by

$$-\rho\overline{u_i' u_j'} = 2\mu_t S_{ij} - \frac{2}{3}\rho k \delta_{ij} \qquad (9)$$

where

$$\mu_t = C_\mu \rho \frac{k^2}{\varepsilon}; S_{ij} = \frac{1}{2}\left(\frac{\partial u_i}{\partial x_j} + \frac{\partial u_j}{\partial x_i}\right) \qquad (10)$$

S_{ij} is the mean rate of strain tensor. The eddy viscosity is related to the turbulent kinetic energy and its dissipation rate. The turbulent kinetic energy k and its dissipation rate ε satisfy the following transport equations within the flow domain:

$$\frac{\partial(\alpha\rho u_j k)}{\partial x_j} = \frac{\partial}{\partial x_j}\left[\alpha(\mu + \frac{\mu}{\sigma_k})\frac{\partial k}{\partial x_j}\right] + 2\alpha\mu_t S_{ij} S_{ij} - \alpha\rho\varepsilon \qquad (11)$$

$$\frac{\partial(\alpha\rho u_j \varepsilon)}{\partial x_j} = \frac{\partial}{\partial x_j}\left[\alpha(\mu + \frac{\mu_t}{\sigma_\varepsilon})\frac{\partial \varepsilon}{\partial x_j}\right] + 2\alpha\mu_t \frac{C_{\varepsilon 1}\varepsilon}{k} S_{ij} S_{ij} - C_{\varepsilon 2}\alpha\rho\frac{\varepsilon^2}{k} \qquad (12)$$

The model coefficients are as follows: C_μ=0.09, $C_{\varepsilon 1}$=1.44, $C_{\varepsilon 2}$=1.92, σ_k=1.0, and σ_ε= 1.3.

Boundary Conditions

At the injection nozzle exit, a constant gas velocity is assumed, and a corresponding source term is added to the axial momentum equation. The liquid volume fraction is set to a value close to unity and the gas volume fraction, close to zero at the beginning of calculations. Along the axis, symmetry conditions are applied, i.e., the radial derivatives of all variables are set to zero except that the mean radial velocities of both phases are set to zero. Along the wall, the velocities satisfy the no-slip condition. The free surface is assumed to be flat, however, the gas bubbles, but not the molten metal, is allowed to freely flow out. This is realised by that a sink term is added to the dispersed (gas) conservation equations for those control volumes at the free surface.

Numerical Procedures

The CFX-4.2 (AEA, 1997) is used to solve the governing equations, along with the boundary conditions. The CFX code is a program for predicting laminar and turbulent flow, and heat transfer, together with additional models such as multi-phase flows, combustion and particle transport.

Trial calculations were conducted to determine the mesh-independent solutions. Three different mesh combinations, 31×26, 62×53, and 122×100 were used. It was found that the mesh combinations 62×53, and 122×100 produced quite similar results (the relative difference between them for all variables is smaller than 0.8%). The non-uniform mesh of 62×53 in axial and radial directions was thus chosen for all the following computations. The false time step was adapted to obtain a converged solution. The converged solution was assumed when the scaled residuals of all the variables were smaller than 10^{-3}.

RESULTS AND DISCUSSION

Simulations are carried out for flows in a model ladle with the liquid Wood's metal agitated by centrally-injected nitrogen at the bottom, using an Eulerian approach. For the cases considered, the bubble Reynolds number is estimated Re=1.56×10^4 (for d_b=0.02 m and the relative velocity between phases is expected to be 0.35 m/s), so the flow is in turbulent region. Three different drag coefficients are examined: C_D=0.44 for spherical particles; C_D=8/3 for spherical cap shaped bubbles because the experimental evidences show that in liquid metals, the bubbles are rather large (for the present case the mean diameter of the bubble is 20 mm) and take on spherical cap shaped; and accounting for the fact that the bubbles may be distorted in the turbulent region, the following relation is also examined (Harmathy, 1960)

$$C_D = \frac{2}{3} E_o^{1/2} \qquad (13)$$

where $E_o = \dfrac{g(\rho_l - \rho_g)d_b^2}{\sigma}$ is the Eotvos number. The mean bubble diameter is set to d_b=0.02 m, which is consistent with the volume/surface mean bubble diameter of the measurements (Xie et al., 1992b). Another mean bubble diameter d_b=0.006 m is also assumed in order to examine the effect of the bubble diameter on the flow. To

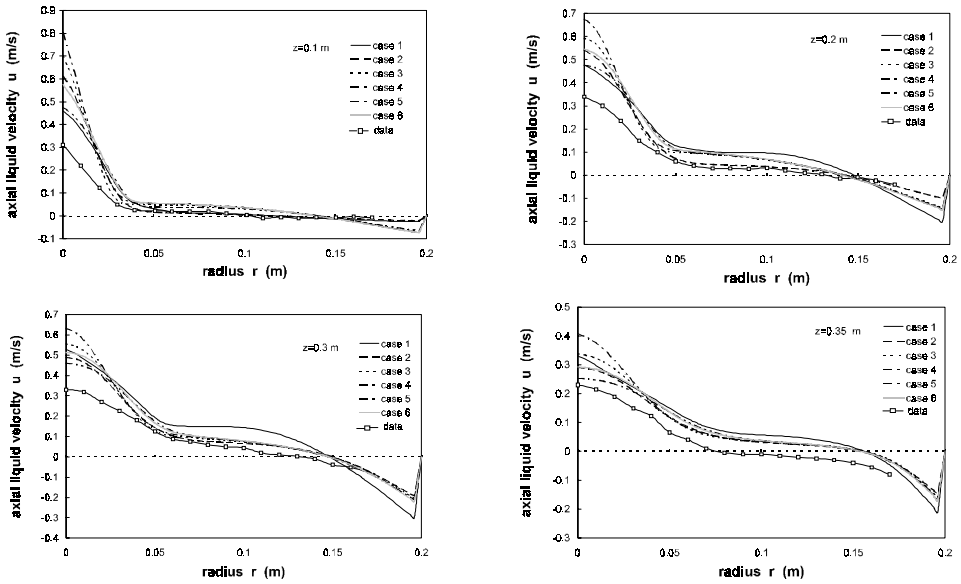

Figure 2: Comparison of predicted axial liquid velocity profiles with experimental data (Xie et al., 1992) at various heights

Table 1 The cases considered

case	C_L	C_{TD}	C_D	d_b (m)	notes
1	0.15	0.1	0.44	0.02	spherical bubbles
2	0.15	0.1	8/3	0.02	spherical cap-shaped bubbles
3	0.1	0.1	0.44	0.006	spherical bubbles
4	0.15	0.1	$\frac{2}{3}Eo^{0.5}$	0.02	distorted bubbles
5	0.3	0.1	8/3	0.02	spherical cap-shaped bubbles
6	0.3	0.1	$\frac{2}{3}(\frac{Eo}{3})^{0.5}$	0.02	proposed drag coefficient

find out the best combination of the coefficients in the interface momentum exchange terms, the lift force coefficient is also changed. Three lift force coefficients (C_L=0.1, 0.15, and 0.3) have been examined. For all the cases, the turbulent dispersion coefficient C_{TD} is set to 0.1. Table 1 lists six typical cases considered.

Figure 2 shows comparison of the predicted axial liquid velocities at four different heights for six different cases, along with the measured data from Xie et al. (1992a). It is seen that all the models reveal the correct trend of the axial liquid velocity distributions. Agreement between predictions and experimental data is relatively reasonable in the liquid region, while a large difference appears in the gas-liquid plume region. Generally all the models overpredict the measured values of the axial liquid velocity in both inside and outside of the gas-liquid plume region. It can also be seen that predictions for the axial liquid velocity outside the gas-liquid plume region are fairly close for all the models except that of case 1. This means that, within the range considered, varying the average bubble diameter, the drag and lift force coefficients do not affect drastically the prediction of the axial liquid velocity in the liquid region. However, the predictions within the gas-liquid plume region are very sensitive to the average bubble diameter, the drag and lift force coefficients used. Case 1 (C_L=0.15, C_D=0.44, and d_b=0.02 m) gives the worst prediction to the axial liquid velocity though at z=0.1 m, it gives nearly the same axial liquid velocity as the experiment. It appears that the drag coefficient for solid particles (C_D=0.44, case 1) is not suitable to be used for modelling flows in molten metals; The distorted particle regime correlation (Harmathy' correlation, case 4) will give too large axial liquid velocity in the plume region and too low bubble rising velocity in the range of off-center plume region, as can be seen later, should thus be inappropriate to be used; For the cases considered, the drag coefficient for spherical cap regime (case 2) may be preferable and gives better predictions to the flow field. Larger lift force coefficient may improve the prediction of the axial liquid velocity in the gas-liquid plume region, comparing between case 2 and case 5. It appears that the relation for the drag coefficient needs to be modified to obtain more reasonable prediction. Based on the trial calculations, we propose the following correlation for the drag coefficient (case 6):

$$C_D = \frac{2\sqrt{3}}{9} E_o^{1/2} \tag{14}$$

With the use of above suggested correlation, the prediction for the liquid velocities and the bubble rising velocity can be improved somewhat.

Comparison of the radial liquid velocity, along with the Xie et al's experimental data, is shown in Fig. 3 at z=0.1 m and z=0.35 m (near the free surface). The dependence of the radial liquid velocity on the radius is quite marked with different models. Predictions reveal reasonable change of the radial liquid velocity with the radius. Near

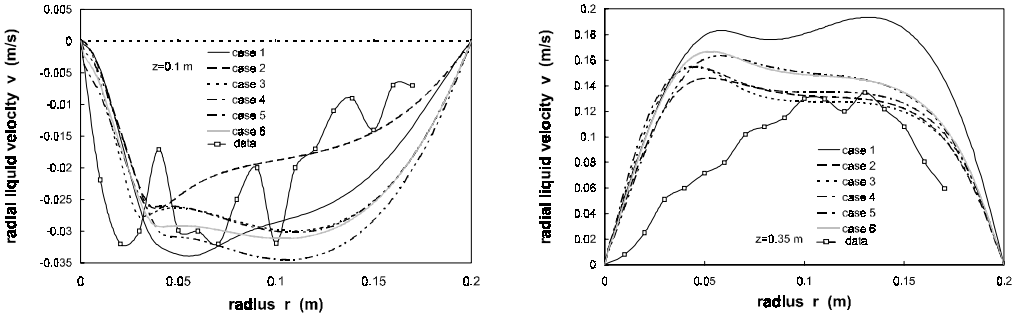

Figure 3: Comparison of predicted radial liquid velocity profiles with experimental data (Xie et al., 1992)

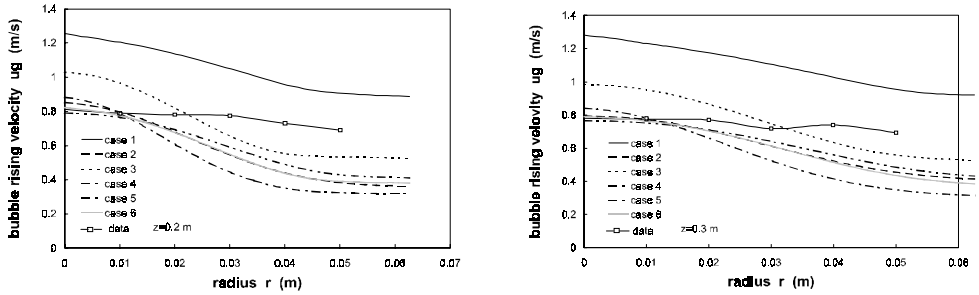

Figure 4: Radial profiles of average bubble rising velocity

the free surface, all the models give steeper variation of the radial liquid velocity in the plume region, compared with the measured data (Xie et al., 1992a). It should be noted that the radial velocity component is quite small, compared with the axial velocity component.

Figure 4 depicts the change of average bubble rising velocity with the radius. It can be seen that near the plume axis, good agreements between the predictions and the experiments are achieved for cases 2, 4, 5 and 6, while a higher bubble rising velocity in this region is predicted in case 1 and case 3. However, in the off-center region of the plume, all the models (except case 1, which persistently overpredict the bubble rising velocity) predict too low bubble rising velocity. This phenomenon was also revealed by Davidson (1990) who modelled the flows in a bath with air-agitated water system.

The calculated radial profiles of gas volume fraction from three models at various heights are compared with the corresponding experimental data of Xie et al. (1992b) in Fig. 5. As can be seen from Fig. 5, numerical predictions produce a low peak of the gas volume fraction near the central axis, and give consistent trend with the experiments in the off-center plume region. It should be mentioned that at small lift force coefficient (e.g., C_l=0.01), the predicted gas fraction decreases with the radius, not shown in the figure (there does not appear such a low peak, but, the predicted value is much higher than the measured value. Thus, this low peak of gas volume fraction at large lift force coefficient is the solution of the equations). It can also be noted that the predicted radial width of the gas-liquid plume is very close to that from the measurements. Comparing the solutions between case 2 and case 5, we can see that the larger the lift force coefficient, the wider spreading the gas-liquid plume, but, large C_L will worsen the prediction of the gas volume fraction, especially in the vicinity of the axis. When the drag coefficient correlation suggested above (Eq. 14) is used, the prediction can be improved somewhat (case 6).

The average bubble rising velocity along the central axis is represented in Fig. 6 for different models, along with the experimental data. Numerical predictions reveal that most of the initial gas kinetic energy is dispersed in the immediate vicinity of the injection nozzle, and the bubble rising velocity sharply decreases within z<0.015 m. Then, there is a recovery region in which the bubble rising velocity increases slightly, Thereafter at z>0.05 m, the bubble rising velocity at the axis remains nearly constant till z≈0.35 m (close to the free surface). And then, when approaching the free surface, the bubbles decelerate. Excellent agreements between predictions and experiments are achieved for case 5 and case 6, and good agreements are also obtained for case 2 and case 4. However, relatively larger deviation from the measured data is observed for case 1 and case 3 which overpredict the axial bubble velocity. This indicates that the bubble distortion should be taken into account, and the solid particle drag coefficient (C_D=0.44) appears unsuitable to be used in modelling flows in the gas stirred molten metals.

CONCLUSIONS

Numerical study is conducted for two phase flows in a model ladle with the Wood's metal agitated by gas injection. Detailed comparison is made for the flow and the gas-liquid plume characteristics of both liquid and

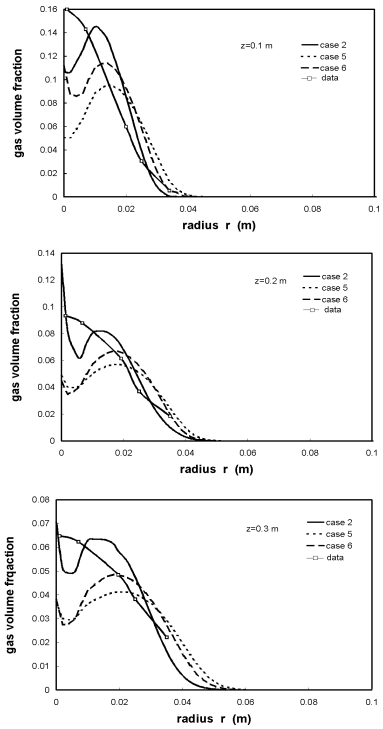

Figure 5 Radial profiles of gas volume fraction at different heights

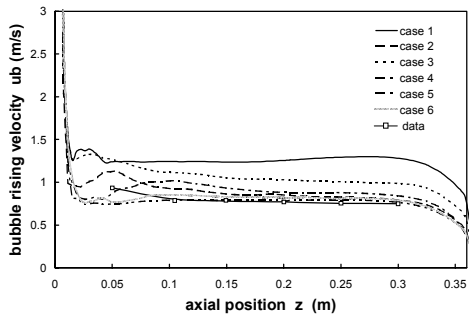

Figure 6 Comparison of predicted bubble rising velocity along the axis with experimental data (Xie et al., 1992)

gas phases. The present results accumulate information of CFD in modelling two phase flows in molten metals.

Among the different correlations of drag coefficient considered, the drag coefficient for spherical cap shaped bubbles is preferable in modelling two phase flows occurring in gas-stirred molten metals. A tentative correlation for the drag coefficient, Eq. (14), which could improve prediction of the flow behaviour, is proposed.

Drag coefficient, lift force coefficient, and their combination are crucial to obtain a reasonable prediction of flows occurring in molten metal systems in using the Eulerian two phase approach. The mathematical model can give reasonable solution to the flow in the liquid region, but, relatively large deviation between predictions and experiments exists in the gas-liquid plume. Improved models are needed for representing the interface interactions.

It is found that for some models, prediction may be reasonable for one phase but not for the other. Thus, comparison between prediction and experimental data should be simultaneously made for flow behaviour of both gas and liquid phases if there exist available data.

REFERENCES

AEA Technology, (1997), "CFX-4.2, Solver Manual", Harwell.

BRIMACOMBE, J. K., NAKANISHI, K., ANAGBO, P. E. and RICHARDS, G. G., (1990), "Process dynamics: gas-liquid", Elliott Symp. Proc., 343.

COOK, T. L. & HARLOW, F. H., (1983), "A computer code for bubbly two phase flow", Report No. LA-10021-MS, Los Alamos National Lab.

DAVIDSON, M. R., (1990), "Numerical calculations of two phase flow in a liquid bath with bottom gas injection: the central plume", Appl. Math. Model., 14, 67.

DREW, D. A. & LAHEY, R. T. Jr., (1987), "The virtual mass and lift force on a sphere in rotating and straining inviscid flow", Int. J. Multiphase Flow, 13(1), 113.

EVANS, J. W., (1997), "Fluid flow in metals processing: Achievements of CFD and opportunities", Int. Conf. On CFD in Mineral and Metal Processing and Power Generation, CSIRO, 7.

HARMATHY, T. Z., (1960), "Velocity of large drops and bubbles in media of infinite and restricted extent", AIChE J., 6, 281.

LAUNDER, B. E. & SPALDING, D. B., (1974), "The Numerical Computation of Turbulent Flow Computer Methods", Appl. Mech. Engng., 3, 269.

LEGENDRE, D. & MAGNAUDET, J., (1998), "The lift force on a spherical bubble in a viscous linear shear flow", J. Fluid Mech., 368, 81.

LOPEZ DE BERTODANO, M., (1992), "Turbulent bubbly two phase flow in a triangular duct", Ph D Thesis, Rensselaer Polytechnic Institute.

MAZUMDAR, D. & GUTHRIE, R. I. L, (1995), "The physical and mathematical modelling of gas stirred ladle systems", ISIJ Int., 35(1) 1-20.

MORI K., (1988), "Kinetics of fundamental reactions pertinent to steelmaking process", Trans. ISIJ, 28, 246.

ORALL, G. & BRIMACOMBE, J. K., (1976) Physical behaviour of a gas jet injected horizontally into liquid metals, Metall. Trans., 7B, 391.

TURKOGLU, H. & FAROUK, B., (1992), "Effect of gas injection velocity on mixing and heat transfer in molten steel baths", Numer. Heat Transfer, 21A, 377.

XIE, Y. & OETERS, F., (1992a), "Experimental studies on the flow velocity of molten metals in a ladle model at centric gas blowing", Steel Research, 63,(3), 93.

XIE, Y., ORSTEN, S., and OETERS, F., (1992b), "Behaviour of bubbles at gas blowing into liquid Wood's metal", ISIJ Int., 32(1), 66.

XIE, Y. & OETERS, F., (1994), "Measurements of bubble plume behaviour and flow velocity in gas stirred liquid Wood's metal with an eccentric nozzle position", Steel Res., 65(8), 315.